Difference in flotation behavior of galena by single and multi-step chronoamperometric oxidation

Orhan Ozdemir [1], Marc A. Hampton [2], Tuan A.H. Nguyen [2], Anh V. Nguyen [2]

[1] Istanbul University-Cerrahpasa, Engineering Faculty, Mining Engineering Department, 34320, Avcilar, Istanbul, Turkey
[2] School of Chemical Engineering, The University of Queensland, Brisbane, Queensland 4072, Australia

Corresponding author: orhanozdemir@istanbul.edu.tr (Orhan Ozdemir), Anh.Nguyen@eng.uq.edu.au (Anh V. Nguyen)

Abstract: The relationship between electrochemical oxidation (Chronoamperometry) of galena surfaces and collocterless galena flotation was investigated in detail. The chronoamperometry (CA) micro-flotation experiments and zeta potential experiments were performed with ground galena particles (106×53 µm). In addition, contact angle measurements were carried out with a freshly cleaved galena sample at pH 4 in order to investigate any changes in galena surface hydrophobicity after the surface oxidation electrochemically. The results from this study indicated that there is a strong link between the nano/micro-physico-chemical properties of a sulphide on galena surfaces and collectorless flotation of galena particles at pH 4. The results were also supported with the electrokinetics behavior and contact angle values of galena particles.

Keywords: surface roughness, hydrophobicity, contact angle, elemental sulfur, galena, chronoamperometry

1. Introduction

A contact of a liquid droplet on a smooth solid surface is controlled by adhesive, capillary and gravitational forces, whose balance affect regime of wetting (De Gennes, 1985; De Coninck et al., 1998; De Gennes et al., 2003; Erbil, 2006; Shikhmurzaev, 2007). It is established that the hydrophobicity (Bauer and Dietrich, 1999; Shikhmurzaev, 2007) and morphology (Cassie and Baxter, 1944; Marmur, 2006; Menges, 2008) of the solid substrate influence significantly the regime of wetting. For this reason, different methods for chemical and morphological (Xia and Whitesides, 1999) pattering of solid substrates were developed recently. Moreover, the hydrophobic surfaces become super-hydrophobic upon the increase of their roughness (Marmur, 2004) due to micro-bubbles trapped into the surface asperities. In addition, complete wetting is possible on super-hydrophobic surfaces via the Cassie-Wenzel wetting regime transitions (Nosonovsky and Bhushan, 2008; Extrand; Forsberg et al.). Except the seminal works of Cassie, Baxter and Young (Cassie and Baxter, 1944; Cassie, 1948; Shikhmurzaev, 1997), the pioneering works of Johnson and Dettre (Johnson and Dettre, 1964; Dettre and Johnson, 1965; Johnson and Dettre, 1966) about the wetting on idealized and non-idealized heterogeneous surfaces should be acknowledged. They established that the surface heterogeneity causes meta-stable configurations of the three-phase contact line.

The shapes of droplets on chemically and morphologically inhomogeneous surface have been studied in the literature (e.g. (Lipowsky et al., 2000; Lipowsky, 2001; Blecua et al., 2006; Quere, 2008). It was established that the chemically heterogeneous surface causes wetting transitions at which the shape of the wetting edge changes in a specific way. If the droplet is substantially larger than the surface patterns the contact angle usually is described by the classical Cassie-Baxter equation. However, if their length-scales are in the same order of magnitude the periodicity of the solid affects the contact angle. For this reason corrections of Cassie-Baxter equations has been made (Wonjae et al., 2009). Detailed

analysis on the problem (Kargupta et al., 2000; Blecua et al., 2006) indicate the existence of contact line contrast and gradients of the intermolecular interactions engendered by the surface inhomogeneity. Flotation is a well-known physico-chemical process depending on surface properties of minerals such as the wettability or hydrophobicity of particles, and the physical characteristics of particles such as size, shape, surface area, roughness, pore size, and structure (Leja, 1982; Chander, 1988; Ulusoy et al., 2003; Nguyen and Schulze, 2004; Kursun, 2009; Ulusoy and Kursun, 2011; Kursun et al., 2018). For instance, the studies on flotation behavior for a liquid partially wetting smooth and rough surfaces showed that the particle surface roughness with sharp protrusions and edges have a significant effect on film thinning and rupture, which affect particle-bubble attachment (Yekeler et al., 2004; Ulusoy and Yekeler, 2005; Koh et al., 2009). Moreover, the critical time of rupture between a bubble and a particle is reduced for particles with rougher surfaces (Verrelli et al., 2014). Another study indicated that there was a strong interaction between bubbles and rough Teflon surfaces while roughness degrees were between 1 µm and 50 µm or more (Krasowska and Malysa, 2007). Finally, nanometer size surface roughness strongly influenced the wetting of hydrophobic materials for both advancing and receding contact angles on the polytetrafluoroethylene (PTFE) films (Miller et al., 1996).

During mining and mechanical processing, minerals are exposed to oxidative environments and the mineral surface oxidizes. An understanding of the oxidative properties of sulphide minerals such as galena (PbS), chalcopyrite ($CuFesS_2$), pyrite (FeS_2), chalcocite (Cu_2S), and bornite (Cu_5FeS_4) is important for effective separation utilizing flotation. Since mineral flotation is the technology of attaching air bubbles to the surfaces of particles in a highly selective manner to separate and concentrate individual mineral components, the particle-bubble attachment is influenced by the particle hydrophobicity, which is known to be a function of the chemical composition and physical morphology (i.e. physicochemical properties) of the particle. Understanding surface oxidation is important for optimizing flotation behavior as the oxidation reaction products can cover the galena particle in a hydrophilic and hydrophobic layer (Richardson, 1995). The later, also known as collectorless flotation, is the focus of this study. In the case galena and other sulphide minerals, it is often stated that oxidation results in a surface coverage of hydrophobic elemental sulphur (Gardner and Woods, 1979; De Giudici et al., 2007). However, previous evidence for elemental sulphur is not conclusive and other theories such as the formation of metal-deficient (Buckley and Riley, 1991) and polysulfide layers (Prince et al., 2002) are still under debate.

As elemental sulphur is hydrophobic, oxidize galena particles can effectively attach to bubble and can be floated without the use of chemical additives. Previous research on collectorless flotation of galena has focused on the sulphur effect, that is, the chemical effect of galena oxidation. However, it is hypothesised that changes in morphology of the galena surface are equally important. It is well known that the physicochemical characteristics of a surface directly influence the hydrophobicity (Bhushan et al., 2009; Chau et al., 2009). It is the link between surface physicochemical properties, hydrophobicity and collectorless flotation that is the focus of this study. A systematic control of the oxidation reaction products and the morphology of these reaction products will improve collectorless flotation and results in a reduction on dependence of flotation chemicals.

Hampton et al used a novel experimental procedure combining Cyclic Voltammetry (CV), Atomic Force Microscopy (AFM) and Raman Spectroscopy, and the results from their studies indicated that the morphology of elemental sulphur on galena surfaces depends on the applied electrochemical potential pathway (Hampton et al., 2011). According to this study, while multi-step CA produced nanoscopic domains on galena surfaces single step caused a layer formation. They also concluded from their studies that these changes on mineral surfaces also changed the hydrophobicity, and hence it would affect the bubble-particle attachment efficiency, hence flotation recovery. In this matter, the aim of this study is to investigate the relationship between electrochemical oxidation of galena surfaces and collocterless galena flotation. The results were also supported with the electrokinetics behavior and contact angle studies of galena particles. The results from this study will be significant to suphide minerals industry so that chemical usage, increase productivity and reduce costs.

2.   Materials and methods

2.1. Materials

A high purity galena (PbS) sample was obtained from Ward's Natural Science (USA). AR grade acetic acid (Rowe Scientific, Australia) and sodium acetate (Sigma-Aldrich, Australia) were used to prepare a pH 4 buffer (0.1 mol/dm^3). Water used in the experiments was freshly purified using a setup consisting of a reverse osmosis RIO's unit and an Ultrapure Academic Milli-Q system (Millipore, USA). The Milli-Q water has a specific resistance of 18.2 MΩcm^{-1}.

2.2. Methods

2.2.1. Electrochemistry experiments

Chronoamperometry (CA) experiments were performed with ground galena particles and a freshly cleaved galena sample in a quiescent pH 4 buffer solution (pre-purged with high purity nitrogen) and a Gamry Reference 600 potentiostat (Gamry, USA). A galena working electrode was connected to the potentiostat working electrode wire using Leit-c-plast (ProSciTech, Australia). A platinum wire was used as a counter electrode and a 3 mol/dm^3 KCl Ag/AgCl microelectrode (Microelectrodes Inc, USA) used as a reference electrode. All voltages are quoted with respect to the Standard Hydrogen Electrode (SHE).

2.2.2. Electrochemical micro-flotation experiments

The micro-flotation tests were carried out using a 250 cm^3 micro-flotation column cell which was mounted on a magnetic stirrer, and a magnetic stirrer bar was used for agitation. In this study, hand-picked pure galena particles were ground using ceramic balls, and sized to 106×53 µm. A 2 g sample was used for each flotation tests. In a typical flotation experiment, first, the reference and counter electrodes were first attached to the electrochemical cell. Then, a suspension of 1% by weight was prepared for the experiments. Finally, the suspension was transferred into the electrochemical cell where nitrogen purged buffer solution, and the CA initiated. The electrochemical cell was enclosed in a nitrogen filled vessel to create a shielding environment. The flotation experiments with multi-step CA were performed successively at +350 mV, +400 mV, +450 mV and +500 mV. Each voltage was held for 300, 900, and 1800 sec, respectively. The coulombs passed per unit area were calculated, and a single step CA performed at +500 mV at until the charge passed per unit area was the same as the multi-step experiment. Therefore, the extent of the reaction in each case will be the same. Once the conditioning was finished, the suspension was transferred to the flotation cell. Finally, the samples were floated for 2 min. using nitrogen at a flow rate of 50 cm^3/min. The galena particles in both float and sink products was determined by gravimetric analysis. An average error of the flotation experiments was about 3%.

2.2.3. Electrochemical zeta potential experiments

Zeta potential measurements of galena particles were carried out using a ZetaPALS instrument utilizing phase analysis light scattering (PALS) technique to determine the electrophoretic mobility of charged suspensions. This technique also allows us to measure the electrophoretic mobility of the particles in salt concentrations up to 3 mol/dm^3. First, about 1 g (<53 µm) of the sample was dry ground using ceramic balls for 15 min. Then, a suspension of 2% by weight was prepared for the experiments, and transferred the electrochemisty cell. In the case of single-step CA, the suspension was kept at 15, 30, 60, and 90 mC, respectively. After this process, the suspension was vacuum filtered, and the dry particles were collected for the zeta potential experiments. Then, the particles were added into DI water, and mixed for 15 min, and the experiments were carried out at different coulombs. In the case of multi-step, the suspension was kept at +350 mV, +400 mV, +450 mV and +500 mV. Each voltage was held for 900 sec, respectively. For pH adjustments, the suspension was mixed for about 5 min in order to reach equilibrium after adding the desired amount of 0.1 M HCl or 0.1 M NaOH. The experiments were carried out at room temperature (22°C). An average error of the zeta potential measurements was ±2-3 mV.

2.2.4. Electrochemical contact angle experiments

Contact angle experiments were performed with a freshly cleaved galena sample in a quiescent pH 4 buffer solution (pre-purged with high purity nitrogen) and a Gamry Reference 600 potentiostat (Gamry, USA). The fresh galena surface was created by cleaving the sample in air using a blade. High purity compressed nitrogen gas was used to remove any loose galena fragments from the surface, the sample was immediately placed in the electrochemical cell and the experiment initiated. In a typical experiment, the reference and counter electrodes were first attached to the electrochemical cell. The fresh galena surface was immediately transferred to the cell, covered with nitrogen purged buffer solution and the CA initiated. The electrochemical cell was enclosed in a nitrogen filled vessel to create a shielding environment. The multi-step CA experiments were performed successively at +350 mV, +400 mV, +450 mV and +500 mV. Each voltage was held for 900 sec. The coulombs passed per unit area were calculated, and a single step CA performed at +500 mV at until the charge passed per unit area was the same as the multi-step experiment.

In a typical experiment, small sessile droplets of 0.5 µL were gently deposited on the galena surface using a precise pipette. A progressive scan CCD camera (model XCD-SX910, Sony, Japan) and a 10× objective (Nikon, Japan) were used to capture the transient images of the evaporating droplet at 15 frames per sec. A fibre light with diffuser was used to illuminate the drop from behind. The videos were then extracted into single images by the Photron Fastcam Viewer 3 software and further analysed using an in-house Matlab code to extract the transient parameters of the droplet geometry. The radius of all the 0.5 µL nanofluid droplets used in this study was much smaller than the capillary length (~2.7 mm), hence the droplet deformation due to gravity was negligible and the detected droplet profiles were perfectly fitted to a circle. An average error of the contact angle experiments was ±3°.

3.   Results and discussion

3.1. Electrochemistry

Multi-step and single-step chronoamperometry data for galena particles is presented in Figs. 1 and 2, respectively. For each flotation experiment, the charge passed per area was kept for each CA test. Therefore, the amount of sulphur on the galena particles would be constant for each flotation test. Figure 1 also shows that nucleation and growth of sulphur domain can be seen from the gathered the CA data, particularly after 400 mV. As already shown from Hampton et al that while nanoscopic domains of sulphur form on the galena surface, layer formation of sulphur takes place on the galena surface (Hampton et al., 2011).

According to Hampton et al, the formation nanoscopic sulphur domains at low anodic potentials and microscopic sulphur domains at higher anodic potentials (Hampton et al., 2011). Particularly the anodic reaction > +200 mV is believed to be due to the formation of elemental sulphur (i.e. oxidation of S^{2-}) and salvation of lead ions Eq. 1:

$$PbS \rightarrow S + Pb^{2+} + 2e^- \tag{1}$$

In-situ AFM tapping mode images taken at the voltages of +8 mV, +258 mV, +308 mV, +358 mV, and +508 mV indicated that the sulphur domains formed on the galena surfaces after the onset of oxidation (+258 mV). With further increases in the surface potential (+308 mV and 358 mV) the domains increase in size and the population increase. The domains are thought to be deposits of sulphur formed as a result of reaction 1, which is confirmed by chemicals analysis of ex-situ Raman spectroscopy. The fact that a homogenous layer of sulphur doesn't form, but deposits do, indicate that the sulphur formed during the oxidation process is released from the surface to the solutes and redeposited at energetically favorable sites such as crystal defects or impurity locations. Therefore, it is reasonable to conclude that Reaction 1 occurs in a two-step process described by Eq. 2:

$$PbS \rightarrow (S-)s + Pb^{2+} + e^- \tag{2}$$

where the subscript s indicates a sulphur intermediate in solution.
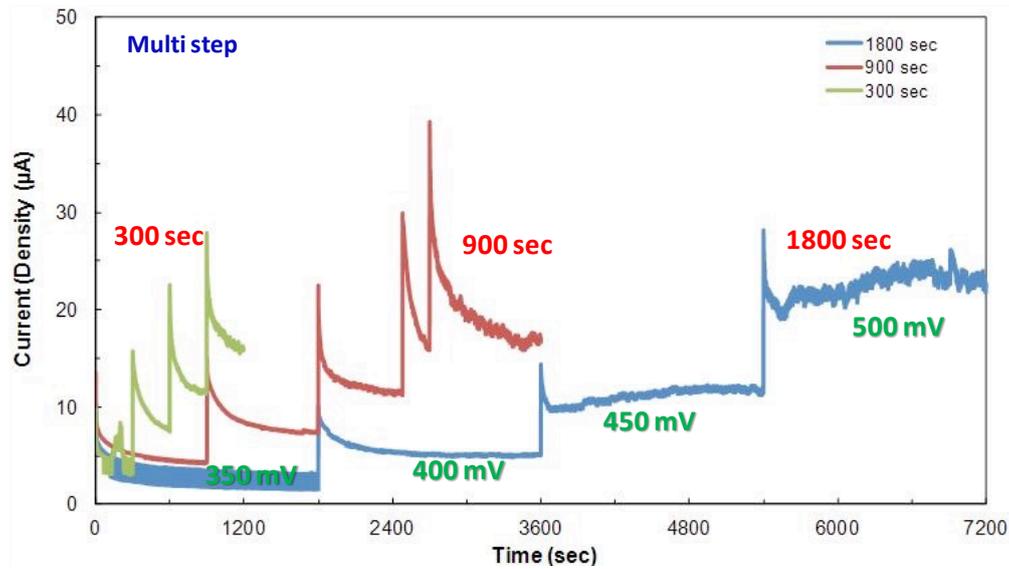
Fig. 1. Multi-step chronoamperometry of galena particles in nitrogen purged pH 4 buffer solution
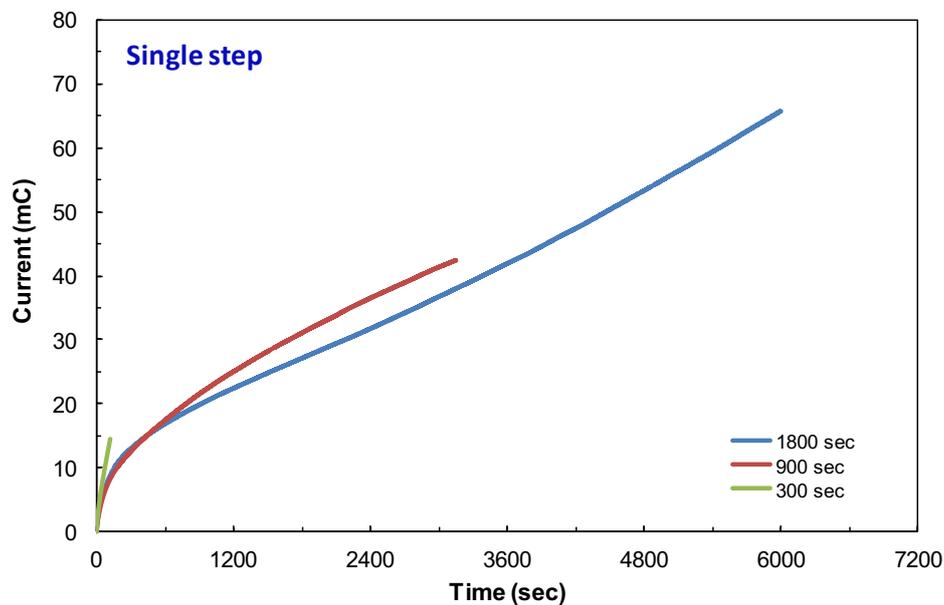
Fig. 2. Single-step chronoamperometry of galena particles in nitrogen purged pH 4 buffer solution

3.2. Electrochemical micro-flotation experiments

The nano/micro scale distribution of oxidation products on the surface and change in morphology may change the physical properties of a surface, hence hdyrophobicity and flotation efficiency. The results from the micro-flotation experiments are shown in Fig. 3. As seen in Fig. 3, as the charge was increased, the flotation recovery also increased. After 20 mC, the rate of recovery was slower and the flotation recovery was constant. Figure 3 also indicates that the flotation recovery of galena is slightly higher than that of single-step.

3.3. Electrochemical zeta potential experiments

Figure 4 shows the zeta potential-pH profile of the galena particles after the CA. As seen from Fig. 4, while the zero point of charge (zpc) of the galena is about pH 6.7, the increase in the charge causes a shift of zpc of the galena particles with an increase in the charge. These results clearly indicate that depending on the growth of sulphur domains in the particles increase the negative charge of particles. Actually, when it is also presented in Fig. 4, the zeta potential-pH profile of elemental sulphur, the

galena particles start behaving as sulphur particle. Figure 5 shows the effect of type of CA on the zeta potential of the particles. As clearly seen from Fig. 5 that the multi-step CA shows more increase on the zeta potential of the galena particles compared to that of single-step. The results of flotation tests were also in line with the results of zeta potential that after applied charge on galena particles showed slightly change on the zeta potential of galena particles.
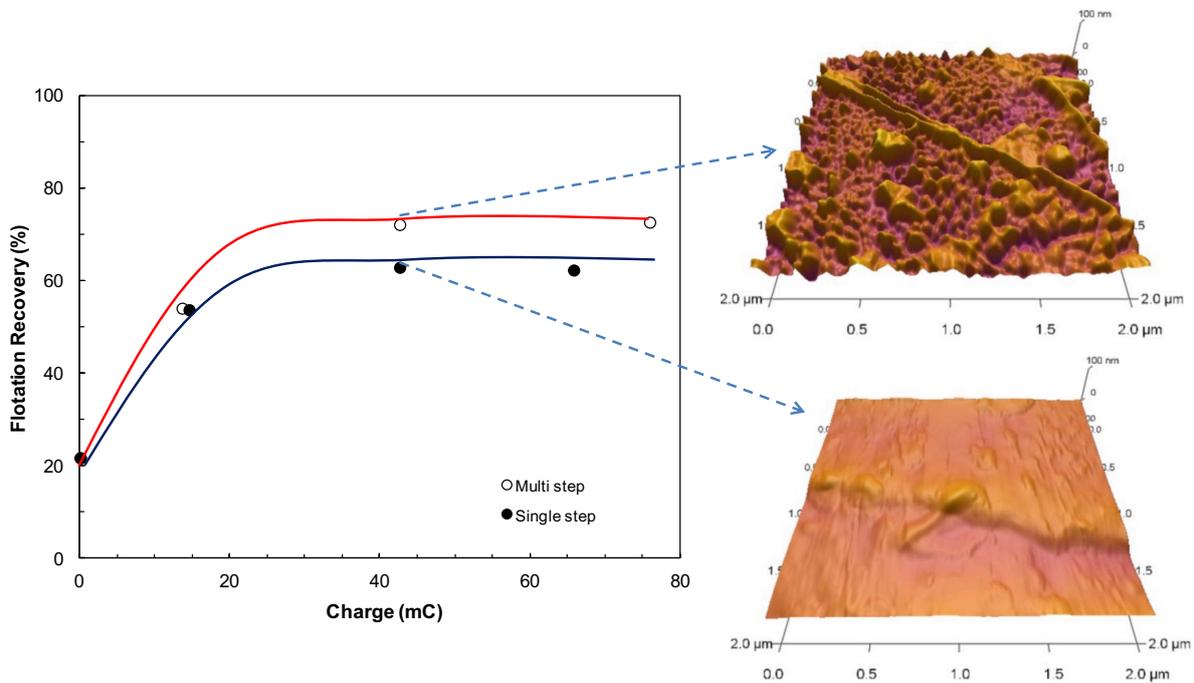
Fig. 3. Micro-flotation results of galena multi-step and single-step CA, and AFM images (Hampton et al., 2012)
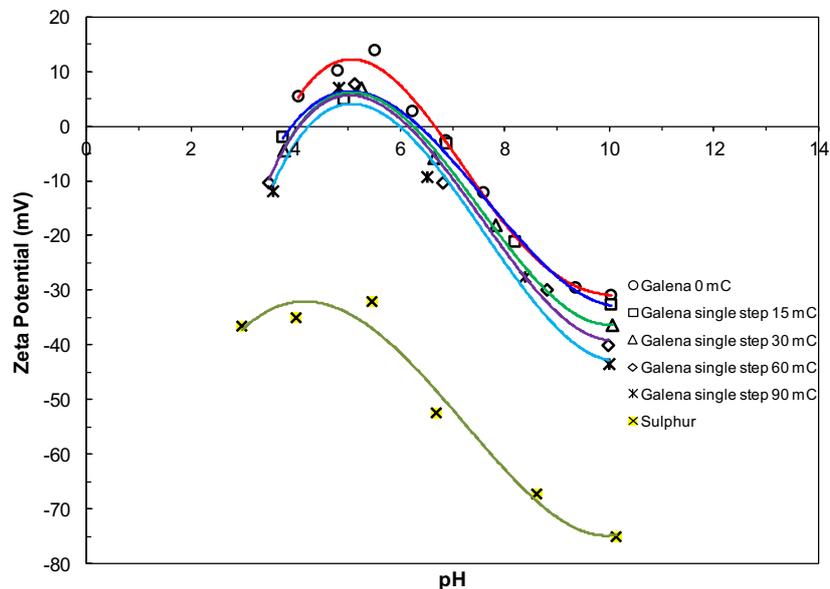
Fig. 4. Zeta potential-pH profile of the galena particles as a function of charge

3.4. Electrochemical contact angle experiments

Wetting phenomena is very important in many applications including flotation. Contact angle measurements and bubble attachment time tests are often used in flotation studies to describe the extent of wetting or the hydrophobicity of a surface. Surface roughness and roughness of different scales has

also been shown to influence contact angle. It is expected that the surface changes will dramatically influence hydrophobicity and thus collectorless flotation. Hydrophobicity dictates flotation. Therefore, an understanding of hydrophobicity and the physic-chemical properties underlying it are of critical importance. Figure 6 shows the contact angles of the galena surfaces after multi-step and single-step CA. As seen from Fig. 6, the contact angle value of galena for multi-step is slightly higher than that of single-step. The advancing contact angle values for each sample are also presented in Table 1. As seen from Table 1, while the contact angle of galena surface for multi-step is 83.5°, it is 73.4° for single-step. Even though there is a slight difference between multi-step and single-step, it is not significant. Meanwhile, it also known from the literature that the advancing contact angle of freshly cleaved is approximately 69°, the receding contact angle was below 10° (Hampton et al., 2012). Based on these results, it can be said that the presence of elemental sulphur considerable increased the contact angle of galena. Figure 7 also shows the microscopic and nanoscopic domains on galena surfaces after multi-step and single-step chronoamperometry.
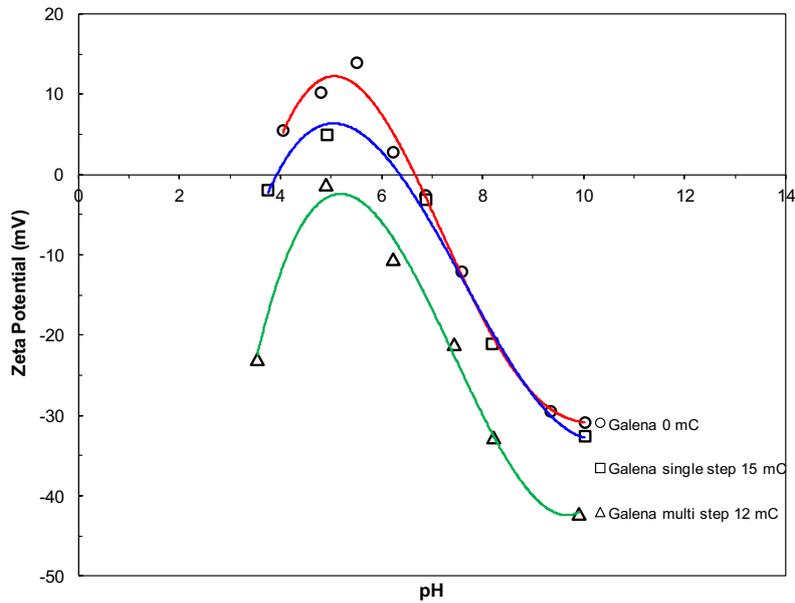
Fig. 5. Effect of type of CA on zeta potential-pH profile of the galena particles
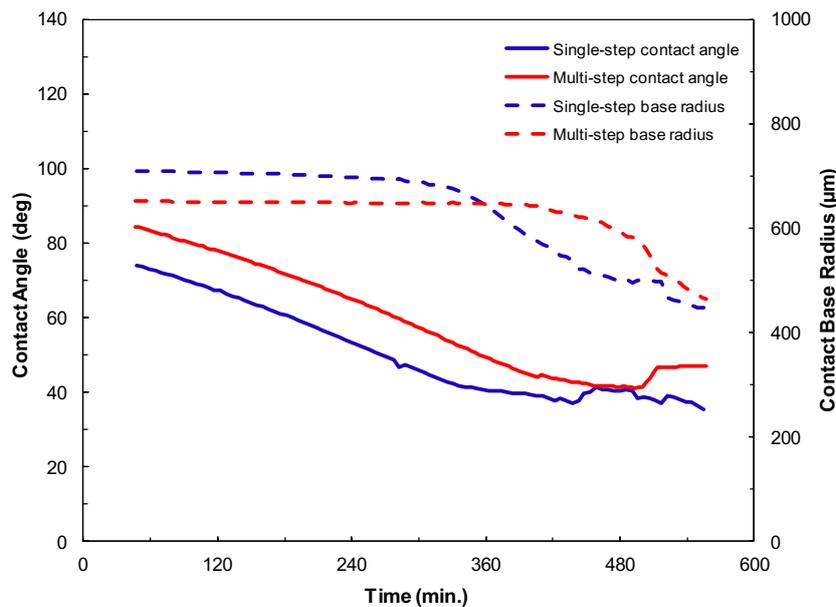
Fig. 6. Contact angle results of galena multi-step and single-step CA

Table 1. Contact angle values for galena particles for multi-step and single-step CA

	Contact Angle (degree)	Error
Multi-step	83.5	1.43
Single-step	73.4	0.6
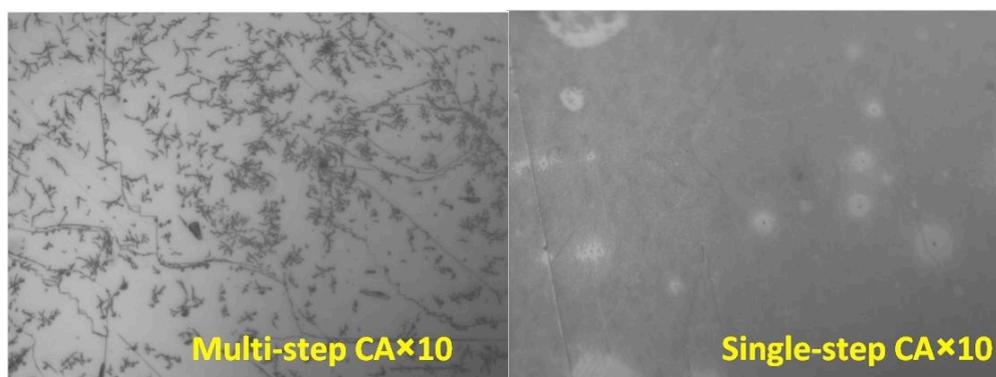
Fig. 7. Microscopic images of galena surfaces covered sulphur domains after multi-step and single-step choronoamperometry

According to these results, the increase in the flotation recovery of galena for multi-step compared to that of single-step is attributed to the considerable changes in the surface morphology due to formation of oxidation species on the galena surfaces. An increase in the number of steps of CA increased the roughness values and hydrophobicity which caused improved flotation recoveries. These findings clearly demonstrated the significance of roughness on the better attachment of particles to the bubbles on flotation process (Ulusoy et al., 2003; Koh et al., 2009; Verrelli et al., 2014).

The increase of the surface roughness usually increases the surface hydrophobicity. For example, the contact angle of water micro-droplets on smooth silica rubber is about 108°, while the contact angle of the same droplets on silicone rubber with micro-roughness is about 135-140°. In the latter case the surface is super-hydrophobic and water repellant - the droplets are rolling on the surface. The reason is that the micro-asperities on the surface trap small air bubbles (air pockets) when the droplet is situated on the surface. These air pockets hold by the micro-asperities of the surface make the surface significantly more hydrophobic because the air bubbles are the most hydrophobic moieties (Larmour et al., 2007).

4.   Conclusions

In this study, the floatability of galena particles after different electrochemical treatments at pH 4 was investigated in detail. Multi-step and single-step chronoamperometry experiments indicated that sulphur formation took place on the galena surfaces. The electrochemical flotation experiments indicated that as the charge was increased, the flotation recovery also increased, and the flotation recovery of galena in the case of multi-step gave slightly higher compared to that of single-step. The results from this study provided a strong link between the nano/micro-physico-chemical properties of a sulphide on mineral surfaces and collectorless flotation. The zeta potential of galena particles showed that the increase in the charge caused a shift of zpc of the galena particles (pH 6.7) with an increase in the charge. Besides, the multi-step CA caused an increase on the zeta potential of the galena particles compared to that of single-step. This can be attributed to the growth of sulphur domains in the particles which increased the negative charge of particles. Additionally, the contact angle measurements were carried out, and the results showed that there was a slightly difference between the galena surfaces for single-step and multi-step prepared. Clearly, the contact angle differences on galena surfaces produced by electrochemical oxidation at pH 4 are chemically and physically heterogeneous because of the presence of pores and cracks, surface roughness. Overall, this study will be significant to the sulphide minerals industry as technological innovations in milling and flotation conditions will increase

productivity and reduce costs. A greater understanding of collectorless flotation will definitely decrease a reliance on flotation chemicals, which has both economic and environmental significance.

Acknowledgments

References

BAUER, C. and DIETRICH, S., 1999. *Wetting films on chemically heterogeneous substrates*, Phys. Rev. E, 60, 6, 6919-6941.

BHUSHAN, B., JUNG, Y.C. and KOCH, K., 2009. *Micro-, nano- and hierarchical structures for superhydrophobicity, self-cleaning and low adhesion*, Philosophical Transactions of the Royal Society A: Mathematical, Physical and Engineering Sciences, 367, 1894, 1631-1672.

BLECUA, P., LIPOWSKY, R. and KIERFELD, J., 2006. *Line tension effects for liquid droplets on circular surface domains*, Langmuir, 22, 26, 11041-11059.

BUCKLEY, A.N. and RILEY, K.W., 1991. *Self-induced floatability of sulphide minerals: Examination of recent evidence for elemental sulphur as the hydrophobic entity*, Surface and Interface Analysis, 17, 9, 655-659.

CASSIE, A.B.D., 1948. Disc. Faraday Soc., 3, 11-19.

CASSIE, A.B.D. and BAXTER, S., 1944. *Wettability of porous surfaces*, Trans. Faraday Soc., 40, 546-550.

CHANDER, S., HOGG, R., 1988. *Physical and surface characterization for mineral processing*, Minerals and Metallurgical Processing152-161.

CHAU, T.T., BRUCKARD, W.J., KOH, P.T.L. and NGUYEN, A.V., 2009. *A review of factors that affect contact angle and implications for flotation practice*, Advances in Colloid and Interface Science, 150, 106-115.

DE CONINCK, J., BLAKE, T.D., CLARKE, A., DE RUIJTER, M.J. and VOUE, M., 1998. *Droplet spreading: A microscopic approach*, Book of Abstracts, 215th ACS National Meeting, Dallas, March 29-April 2COLL-065.

DE GENNES, P.G., 1985. *Wetting: statics and dynamics*, Rev. Mod. Phys., 57, 3, 827-863.

DE GENNES, P.G., BROCHARD-WYART, F. and QUERE, D., 2003. Capillarity and Wetting Phenomena. Berlin, Springer.

DE GIUDICI, G., RICCI, P., LATTANZI, P. and ANEDDA, A., 2007. *Dissolution of the (001) surface of galena: An in situ assessment of surface speciation by fluid-cell micro-Raman spectroscopy*, American Mineralogist, 92, 4, 518-524.

DETTRE, R.H. and JOHNSON, R.E., 1965. *Contact Angle Hysteresis .4. Contact Angle Measurements on Heterogeneous Surfaces*, J. Phys. Chem., 69, 5, 1507-1515.

ERBIL, H.Y., 2006. Surface Chemistry of Solid and Liquid Interfaces. Oxford, Blackwell Publishing.

EXTRAND, C.W., 2011. *Repellency of the Lotus Leaf: Resistance to Water Intrusion under Hydrostatic Pressure*, Langmuir, 27, 11, 6920-6925.

FORSBERG, P., NIKOLAJEFF, F. and KARLSSON, M., 2011. *Cassie-Wenzel and Wenzel-Cassie transitions on immersed superhydrophobic surfaces under hydrostatic pressure*, Soft Matter, 7, 1, 104-109.

GARDNER, J.R. and WOODS, R., 1979. *A study of the surface oxidation of galena using cyclic voltammetry*, Journal of Electroanalytical Chemistry, 100, 1-2, 447-459.

HAMPTON, M.A., PLACKOWSKI, C., BRUCKARD, W.J. and NGUYEN, A.V., 2012. In-situ investigation of sulfide mineral surface oxidation under controlled potential by combined Atomic Force Microscopy and Chronoamperometry, XXVI. International Mineral Processing Congress (IMPC), New Delhi, India,

HAMPTON, M.A., PLACKOWSKI, C. and NGUYEN, A.V., 2011. *Physical and Chemical Analysis of Elemental Sulfur Formation during Galena Surface Oxidation*, Langmuir, 27, 7, 4190-4201.

JOHNSON, R.E. and DETTRE, R.H., 1964. *Contact Angle Hysteresis .3. Study of an Idealized Heterogeneous Surface*, J. Phys. Chem., 68, 7, 1744-1750.

JOHNSON, R.E. and DETTRE, R.H., 1966. *Wettability of Low-Energy Liquid Surfaces*, J Colloid Interface Sci, 21, 6, 610-622.

KARGUPTA, K., KONNUR, R. and SHARMA, A., 2000. *Instability and pattern formation in thin liquid films on chemically heterogeneous substrates*, Langmuir, 16, 26, 10243-10253.

KOH, P.T.L., HAO, F.P., SMITH, L.K., CHAU, T.T. and BRUCKARD, W.J., 2009. *The effect of particle shape and hydrophobicity in flotation*, International Journal of Mineral Processing, 93, 2, 128-134.

KRASOWSKA, M. and MALYSA, K., 2007. *Wetting films in attachment of the colliding bubble*, Advances in Colloid and Interface Science, 134-135, 138-150.

KURSUN, I., 2009. *Particle size and shape characteristics of Kemerburgaz quartz sands obtained by sieving, laser diffraction and digital image processing methods*, Mineral Processing & Extractive Metall. Rev, 30(4), 346-360.

KURSUN, I., TERZI, M., OZDEMIR, O., 2018. *Evaluation of digital image processing (DIP) in analysis of magnetic separation fractions from Na-feldspar ore*, Arabian Journal of Geosciences, 11(16), 462.

LARMOUR, I.A., BELL, S.E., SAUNDERS, G.C., 2007. Remarkably simple fabrication of superhydrophobic surfaces using electroless galvanic deposition, Angew Chem Int Ed Engl., 46, 1710-1712.

LEJA, J., 1982. Surface Chemistry of Froth Flotation. New York, NY, Plenum Press.

LIPOWSKY, R., 2001. *Morphological wetting transitions at chemically structured surfaces*, Curr Opin Colloid Interface Sci., 6, 40-48.

LIPOWSKY, R., LENZ, P. and SWAIN, P.S., 2000. *Wetting and Dewetting of Structured and Imprinted Surfaces*, Colloids Surf., A, 161, 3-22.

MARMUR, A., 2004. *The lotus effect: Superhydrophobicity and metastability*, Langmuir, 20, 9, 3517-3519.

MARMUR, A., 2006. *Underwater Superhydrophobicity: Theoretical Feasibility*, Langmuir, 22, 1400-1402.

MENGES, F.R. (2008). *Wetting of micro- and nanostructured hydrophobic surfaces*. B. Sc., RWTH Aachen University of Technology

MILLER, J.D., VEERAMASUNENI, S., DRELICH, J., YALAMANCHILI, M.R. and YAMAUCHI, G., 1996. *Effect of roughness as determined by atomic force microscopy on the wetting properties of PTFE thin films*, Polym. Eng. Sci., 36, 14, 1849-1855.

NGUYEN, A.V. and SCHULZE, H.J., 2004. Colloidal Science of Flotation. New York, Marcel Dekker.

NOSONOVSKY, M. and BHUSHAN, B., 2008. *Cassie-Wenzel Wetting Regime Transition*. Multiscale Dissipative Mechanisms and Hierarchical Surfaces: Friction, Superhydrophobicity, and Biomimetics**:** 153-167.

PRINCE, K., HEUN, S., GREGORATTI, L., BARINOV, A. and KISKINOVA, M., 2002. *Long-Term Oxidation Behaviour of Lead Sulfide Surfaces Nanoscale Spectroscopy and Its Applications to Semiconductor Research*. Y. Watanabe, G. Salviati, S. Heun and N. Yamamoto, Springer Berlin / Heidelberg. **588:** 111-120.

QUERE, D., 2008. *Wetting and roughness*. Annual Review of Materials Research, Palo Alto, Annual Reviews. **38:** 71-99.

RICHARDSON, P.E., 1995. *Surface Chemistry of Sulfide Flotation*. Mineral Surfaces, D. J. Vaughan and R. A. D. Pattrick, London, Chapman & Hall**:** 261-272.

SHIKHMURZAEV, Y.D., 1997. *Moving Contact Lines in Liquid/Liquid/Solid Systems*, Journal of Fluid Mechanics, 334, 211-249.

SHIKHMURZAEV, Y.D., 2007. Capillary flows with forming interfaces New York, CRC Press.

ULUSOY, U. and YEKELER, M., 2005. *Correlation of the surface roughness of some industrial minerals with their wettability parameters*, Chemical Engineering and Processing: Process Intensification, 44, 5, 555-563.

ULUSOY, U., YEKELER, M. and HIÇYıLMAZ, C., 2003. *Determination of the shape, morphological and wettability properties of quartz and their correlations*, Minerals Engineering, 16, 10, 951-964.

ULUSOY, U., KURŞUN, I., 2011. *Comparison of different 2d image analysis measurement techniques for the shape of talc particles produced by different media milling*, MINERALS ENGINEERING, 24, 91-97.

VERRELLI, D.I., BRUCKARD, W.J., KOH, P.T.L., SCHWARZ, M.P. and FOLLINK, B., 2014. *Particle shape effects in flotation. Part 1: Microscale experimental observations*, Minerals Engineering, 58, 0, 80-89.

WONJAE, C., TUTEJA, A., MABRY, J.M., COHEN, R.E. and MCKINLEY, G.H., 2009. *A modified Cassie–Baxter relationship to explain contact angle hysteresis and anisotropy on non-wetting textured surfaces*, J Colloid Interface Sci, 339, 208-216.

XIA, Y. and WHITESIDES, G.M., 1999. *Soft Lithography*, Annu. Rev. Mater. Sci., 28, 153-184.

YEKELER, M., ULUSOY, U. and HIÇYıLMAZ, C., 2004. *Effect of particle shape and roughness of talc mineral ground by different mills on the wettability and floatability*, Powder Technology, 140, 1-2, 68-78.